CHAPTER 4

STEADY STATE ANALYSIS AND SIMULATION OF THE IPM GENERATOR

FEEDING A RECTIFIER-RESISTIVE LOAD

4.1 Introduction

In this chapter, steady state analysis and simulation analysis will be performed upon the IPM generator feeding a rectifier-resistive load. The rectifier is at the heart of the buck and boost topologies (which will be presented in the next two chapters) as well, and, thus, the results of the derivations and simulation procedures developed here will also be used in the next two chapters.

The first part of the chapter concerns itself with developing mathematical equations which describe the   switching functions of the rectifier-resistive load under steady state. The model developed uses switching function theory [33] to convert the rectifier-resistive load into an equivalent resistance.

Next, using the mathematical model developed, the steady state experimental results will be compared with the predicted results. It will be seen that the predicted performance of the terminal voltage and output power is higher than the experimental results. This is due largely to the fact that the mathematical model of the rectifier ignores commutation overlap, and only the fundamental component of the switching function is used. Nevertheless, the predicted performance is relatively close to the experimental results, and the mathematical models are definitely useful in showing the trend of how the system will operate

The second half of the chapter concerns itself with simulating the IPM generator feeding the rectifier-resistive load. The method used to simulate the rectifier will be explained. The diode, which is the component that makes up the rectifier, is a somewhat difficult device to model because the passive way in which it turns on and off. The switch is not externally (user) controlled; rather, it is dependent upon the voltage across it and the current flowing through it. The model of the diode (along with the models of the inductor and capacitor) will be explained and then the topology of a full bridge rectifier and filter feeding a resistive load will be simulated for the case when an ideal voltage source is acting as the power source.

The remaining part of the chapter will compare the simulated and measured waveforms when the IPM generator is feeding the rectifier-resistive load. Three cases will be examined. The first case is for a heavy load where the output power of the generator is near its maximum point for a particular operating frequency (45 Hz). The second and third cases examine the measured and simulated waveforms for the case of a very light load. The difference between the second and third cases is the value of the rectifier filter capacitor. In the second case, the filter capacitor is 5.6 μF and in the third case it is 11.2 μF. It will be seen that the effect of raising the filter capacitor causes the IPM-rectifier-resistive scheme to go from the stable nonoscillatory mode depicted in the second case to a quasi-periodic oscillatory mode for the third case.

4.2 Derivation for Rectifier in Steady State

The model of the generator-diode-rectifier load system is shown in Figure 4.1. Using the concept of existence function to represent the rectifier switching operation, the current and voltage relationships between input and output of the three-phase diode rectifier can be expressed as

$$
\begin{aligned}
I_{ar} &= S_a I_d \\
I_{br} &= S_b I_d \\
I_{cr} &= S_c I_d \ ,
\end{aligned}
\tag{4.1}
$$

and

$$
V_d = S_a V_{as} + S_b V_{bs} + S_c V_{cs} \ .
\tag{4.2}
$$

These two equations can be used to find an equivalent resistance which can be used to represent a rectifier.

The switching functions $S_{a,b,c}$ are given as

$$
\begin{aligned}
S_a &= A_n \cos(\omega_e t) \\
S_b &= A_n \cos(\omega_e t - \frac{2\pi}{3}) \\
S_c &= A_n \cos(\omega_e t + \frac{2\pi}{3}) \ ,
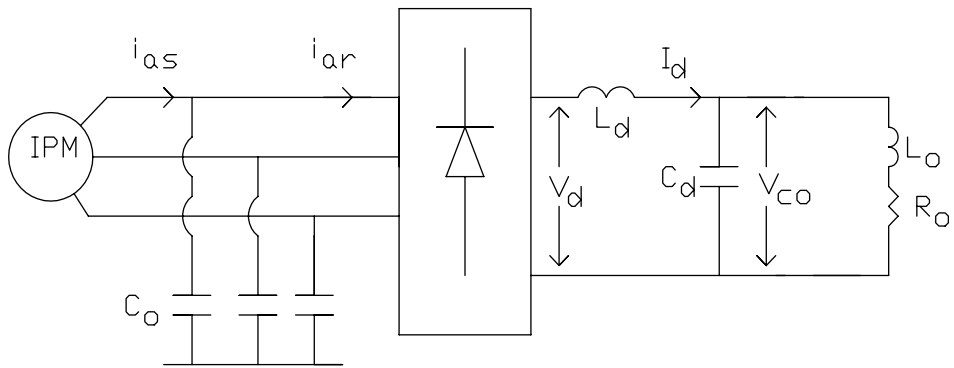\end{aligned}
\tag{4.3}
$$

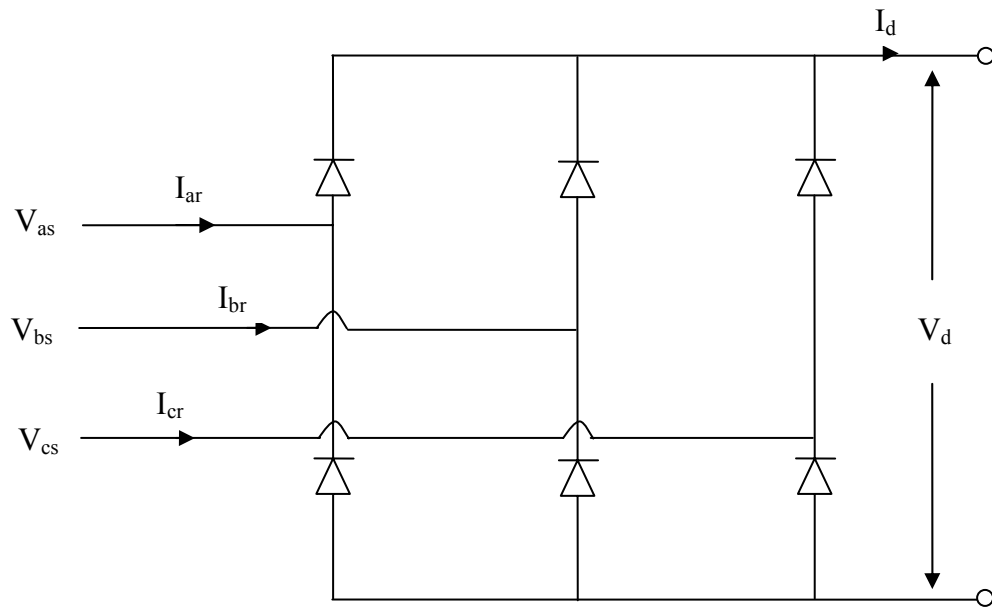Figure 4.1 Schematic diagram of IPM-Rectifier feeding an impedance load

Figure 4.2. Schematic diagram of 3 phase full bridge rectifier

where

$$A_n = \frac{4}{\pi} \frac{1}{n} \sin(\frac{n\pi}{2}) \cos(\frac{n\pi}{6}) \ .$$

Therefore, for the first harmonic A_1 (n=1) gives

$$A_1 = \frac{4}{\pi} \cos\frac{\pi}{6} = \frac{2\sqrt{3}}{\pi} \ . \qquad (4.4)$$

Thus, if only the fundamental frequency is considered, the switching functions can be written as

$$S_a = A_1 \cos(\omega_e t)$$
$$S_b = A_1 \cos(\omega_e t - \frac{2\pi}{3}) \qquad (4.5)$$
$$S_c = A_1 \cos(\omega_e t + \frac{2\pi}{3}) \ .$$

In order to remove time as a variable in the switching function equations (and the state equations), the equations will be transformed from the abc reference frame to the dqo reference frame.

$$\begin{bmatrix} S_q \\ S_d \\ S_o \end{bmatrix} = [T(\theta)] \begin{bmatrix} S_a \\ S_b \\ S_c \end{bmatrix} , \qquad (4.6)$$

where

$$T(\theta) = \frac{2}{3} \begin{bmatrix} \cos(\theta) & \cos(\theta - \frac{2\pi}{3}) & \cos(\theta + \frac{2\pi}{3}) \\ \sin(\theta) & \sin(\theta - \frac{2\pi}{3}) & \sin(\theta + \frac{2\pi}{3}) \\ \frac{1}{2} & \frac{1}{2} & \frac{1}{2} \end{bmatrix} .$$

In this analysis, it is assumed that generator voltages and currents are balanced. With this assumption, it is correct to say that the zero sequence components (o of dqo terms) is zero. With this in mind, the switching functions given in Equation (4.5) can be written in the dq reference frame as

$$\begin{aligned} S_q &= A_1 \cos(\omega t - \theta) \\ S_d &= -A_1 \sin(\omega t - \theta), \end{aligned} \tag{4.7}$$

where, in the synchronously rotating reference frame

$$\theta = (\omega t + \delta),$$

and the term δ is the initial torque angle of the source generator.

Thus, substituting Equation (4.4) into (4.7), the switching functions in the synchronously rotating reference frame can be written as

$$S_q = \frac{2\sqrt{3}}{\pi} \cos(-\delta) = \frac{2\sqrt{3}}{\pi} \cos(\delta)$$

$$S_d = -\frac{2\sqrt{3}}{\pi} \sin(-\delta) = \frac{2\sqrt{3}}{\pi} \sin(\delta).$$

(4.8)

The currents going into the rectifier can now be written in the dq reference frame as

$$i_{qr} = S_q I_d$$
$$i_{dr} = S_d I_d ,$$

(4.9)

and the dc voltage out of the rectifier is

$$V_d = S_q V_{qs} + S_d V_{ds} .$$

(4.10)

The state equations of the system can be found as follows.

For the ac capacitor,

$$C_0 \frac{dV_{as}}{dt} = i_{as} - i_{ar}$$

$$C_0 \frac{dV_{bs}}{dt} = i_{bs} - i_{br}$$

$$C_0 \frac{dV_{cs}}{dt} = i_{as} - i_{cr} ,$$

(4.11)

for the filter inductor L_d ,

$$L_d \frac{dI_d}{dt} = V_d - V_{co} ,$$

(4.12)

for the filter capacitor C_d ,

$$C_d \frac{dV_{co}}{dt} = I_d - I_o \ ,$$

$$(4.13)$$

and for the load inductor L_o ,

$$L_o \frac{dI_o}{dt} = V_{co} - R_o I_o \ .$$

$$(4.14)$$

The state equations also need to be transformed into the dq reference frame; however, the only states which are not dc quantities are the three equations of the ac capacitor. The dq transformation of Equation (4.11) gives

$$C_0 \frac{dV_{qs}}{dt} = (i_{qs} - i_{qr}) - \omega C_0 V_{ds}$$

$$C_0 \frac{dV_{ds}}{dt} = (i_{ds} - i_{dr}) + \omega C_0 V_{qs} \ .$$

$$(4.15)$$

With the above state equations, it is now possible to substitute the currents i_{qr} and i_{dr} in terms of the rectifier current I_d and the rectifier voltage V_d in terms of the input voltages of the rectifier V_{qs} and V_{ds}. The ultimate purpose of this is to derive a steady state model of the rectifier which can be represented simply as an equivalent (thevenin) resistance. Before any substitutions are made however, the differential equations will be reduced to their steady state models (meaning that, since, at steady state, the rate of change of the states is zero, the left side of the equations becomes equal to zero).

Thus, Equations (4.12 - 4.15) at steady state are

$$0 = V_d - V_{co}$$
$$0 = I_d - I_o$$
$$0 = V_{co} - R_o I_o \qquad (4.16)$$
$$0 = i_{qs} - i_{qr} - \omega C_o V_{ds}$$
$$0 = i_{ds} - i_{dr} + \omega C_o V_{qs} \ .$$

Therefore,

$$V_d = V_{co} = R_o I_o = R_o I_d \ , \qquad (4.17)$$

or

$$I_d = \frac{V_d}{R_o} \ . \qquad (4.18)$$

This gives the equivalent resistance on the load side of the rectifier; but the objective is to obtain an equivalent resistance on the source side of the rectifier. In order to accomplish this goal, two manipulations will be made. The first is to let the ac capacitance C_o approach a zero value. With this constraint:

$$As \ C_0 \to 0$$
$$0 = i_{qs} - i_{qr} \qquad (4.19)$$
$$0 = i_{ds} - i_{dr} \ .$$

Therefore,

$$i_{qs} = i_{qr}$$
$$i_{ds} = i_{dr} \ . \qquad (4.20)$$

The switching function equations relating the dc current to the ac currents can be written as

$$i_{qs} = S_q I_d$$
$$i_{ds} = S_d I_d \ .$$

(4.21)

The second manipulation is to place the desired equivalent resistance R_{eq} into the dq reference frame giving

$$V_{qs} = R_{eq} i_{qs}$$
$$V_{ds} = R_{eq} i_{ds} \ .$$

(4.22)

With these two manipulations made, the derivation for an equivalent resistance representing the rectifier is possible, and is as follows.

From Equation (4.21),

$$I_d = \frac{i_{qs}}{S_q} = \frac{i_{ds}}{S_d} \ ,$$

(4.23)

so

$$i_{ds} = \frac{S_d}{S_q} i_{qs} \ .$$

(4.24)

Combining the results of Equations (4.22) and (4.24) gives

$$V_{ds} = R_{eq} i_{ds} = R_{eq} \frac{S_d}{S_q} i_{qs} \, . \tag{4.25}$$

Substituting the results of Equation (4.25) and (4.17) into Equation (4.10) gives

$$S_q V_{qs} + S_d \left(\frac{S_d}{S_q} i_{qs} R_{eq} \right) = V_d = I_d R_o = \frac{R_o i_{qs}}{S_q} \, , \tag{4.26}$$

or

$$S_q V_{qs} = i_{qs} \left(\frac{R_o}{S_q} - \frac{S_d^2}{S_q} R_{eq} \right) = \frac{V_{qs}}{R_{eq}} \left(\frac{R_o}{S_q} - \frac{S_d^2}{S_q} R_{eq} \right) \, . \tag{4.27}$$

Rearranging gives

$$R_{eq} \left(S_q + \frac{S_d^2}{S_q} \right) = \frac{R_o}{S_q} \, . \tag{4.28}$$

Therefore, the equivalent resistance can be written as

$$R_{eq} = \frac{R_o}{S_q^2 + S_d^2} \, . \tag{4.29}$$

Substituting the values found for the switching functions S_q and S_d given in Equation (4.8) gives

$$R_{eq} = \frac{R_o}{A_1^2 \cos^2 \delta + A_1^2 \sin^2 \delta} = \frac{Ro}{A_1^2} \quad . \tag{4.30}$$

Finally, substituting the numeric value for A_1 gives the final result as

$$R_{eq} = \frac{\pi^2 R_o}{12} \quad . \tag{4.31}$$

Thus, Equation (4.31) is saying that a 100 Ω rectifier resistance R_O would appear to the generator as a balanced, three-phase resistance having a value of approximately 83 Ω.

4.3 Steady State Performance of an IPM Generator Feeding a Rectifier-Resistive Load

In this section, the predicted performance curves obtained by using the procedure outlined in section 4.2 will be compared with the steady state experimental measurements for the case when the IPM is feeding a rectifier-resistive load.
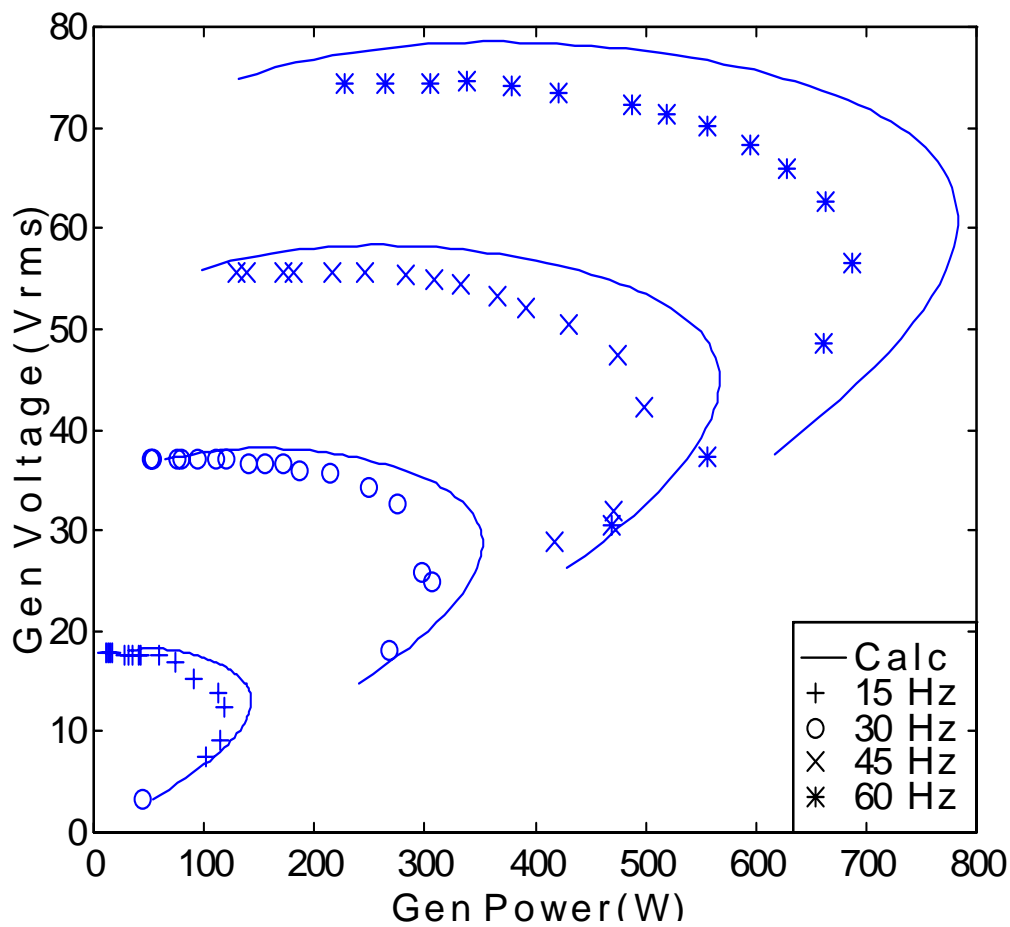
Figure 4.3. Measured and calculated line to neutral voltage vs output power for IPM machine

Figure 4.3 shows the plot of generator line to neutral voltage vs the output power of the generator for four different operating frequencies. The graph indirectly shows the disadvantage of assuming that no commutation overlap is occurring and that the rectifier can be modeled as a resistive load because, if the rectifier truly represented a pure resistance to the generator, then the measured output voltage and generator power would fall on the predicted performance line as closely as those of Figure 3.5.
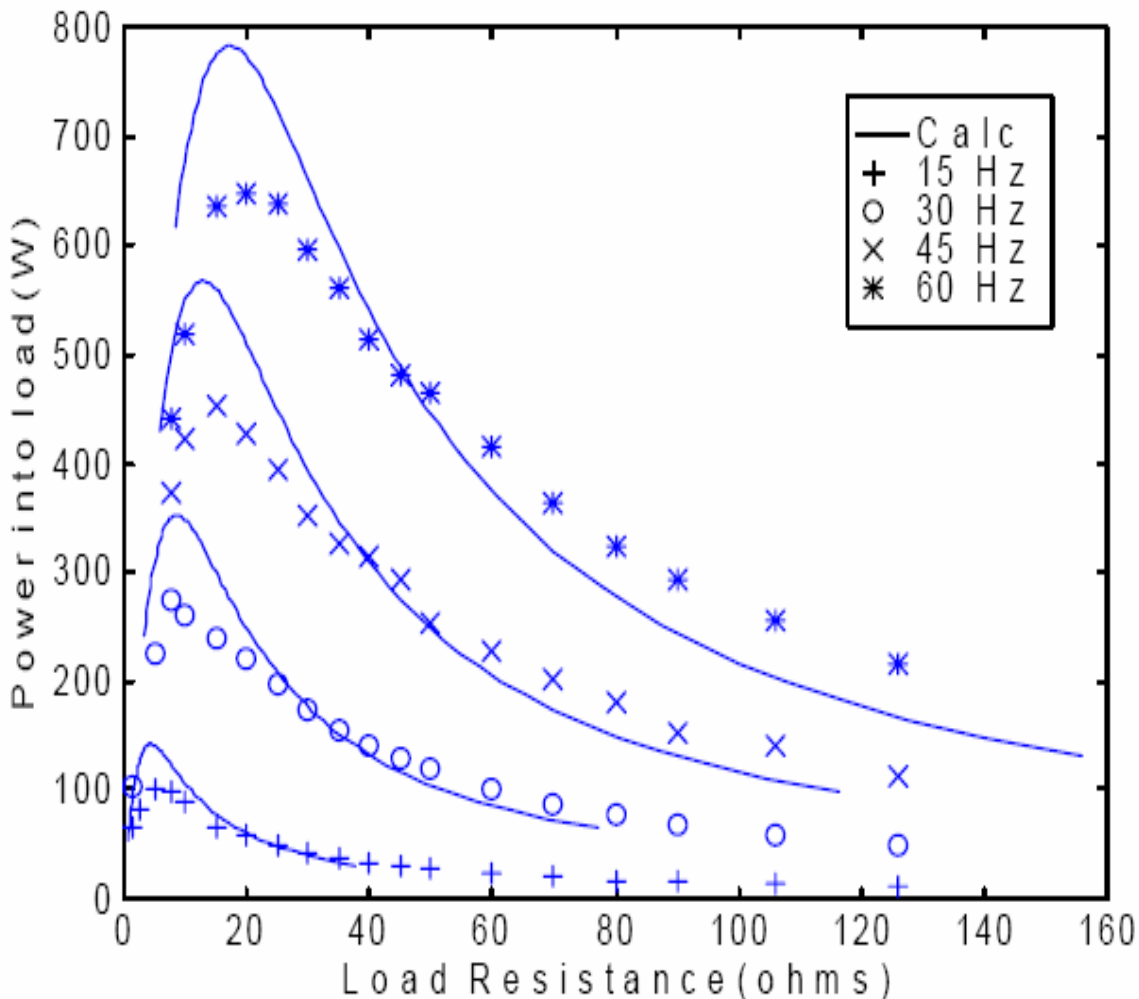
Figure 4.4. Measured and calculated load power vs load resistance for IPM feeding a rectifier-resistive load

Figure 4.4 shows the graph of the measured and calculated output power vs the load resistance. It can be seen that the predicted performance curves show the trend of the actual measured points, but there is a fairly substantial magnitude difference in output power between the predicted and measured curves.

Figure 4.5 plots the load voltage vs the generator current. It can be seen that measured and calculated curves follow each other closely until the generator current becomes very small. When this occurs, the mathematical model predicts that the load voltage will drop fairly rapidly, while the measured values suggest that the load voltage will
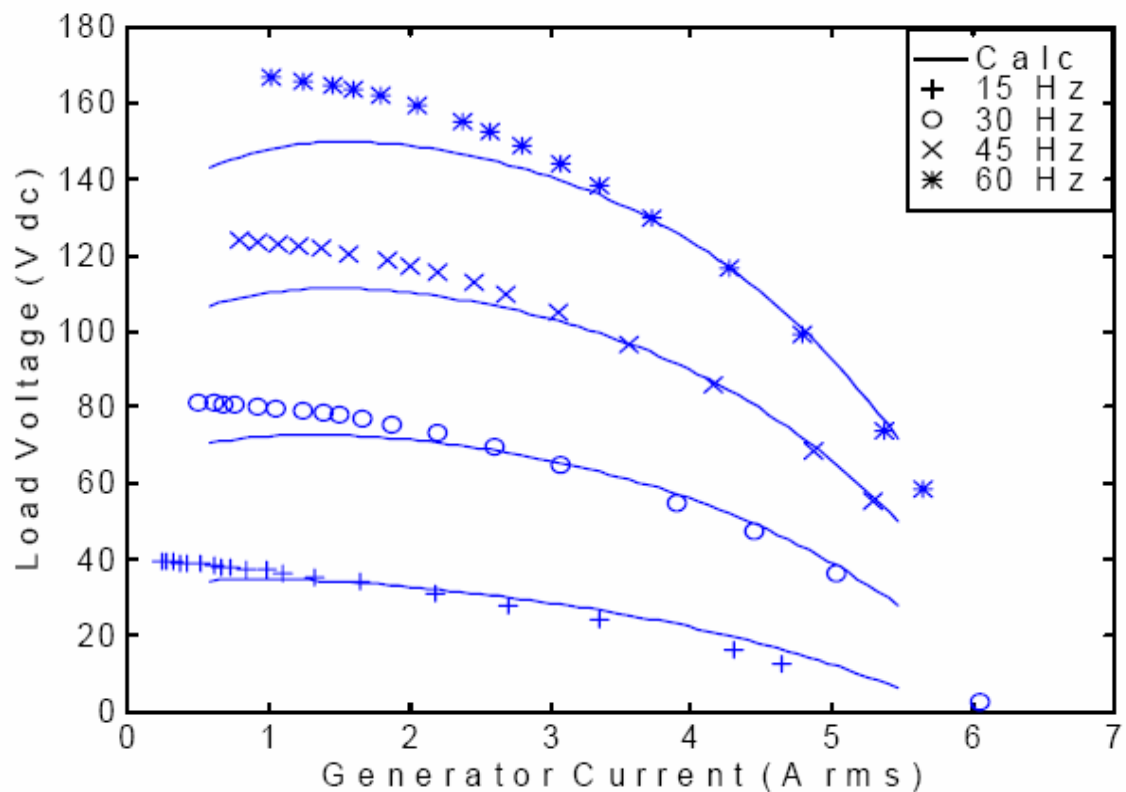
Figure 4.5. Measured and calculated load voltage vs generator current for IPM feeding a rectifier-resistive load

level off, but not drop as the stator current decreases (which is due to the load resistance increasing).

The graph shown in Figure 4.6 displays the load voltage vs the generator power characteristics. The maximum measured power out of the generator is approximately 690 watts at 60 Hz operation, as compared to approximately 780 watts generator output power for the case of a resistive load at 60 Hz (see Figure 3.5).
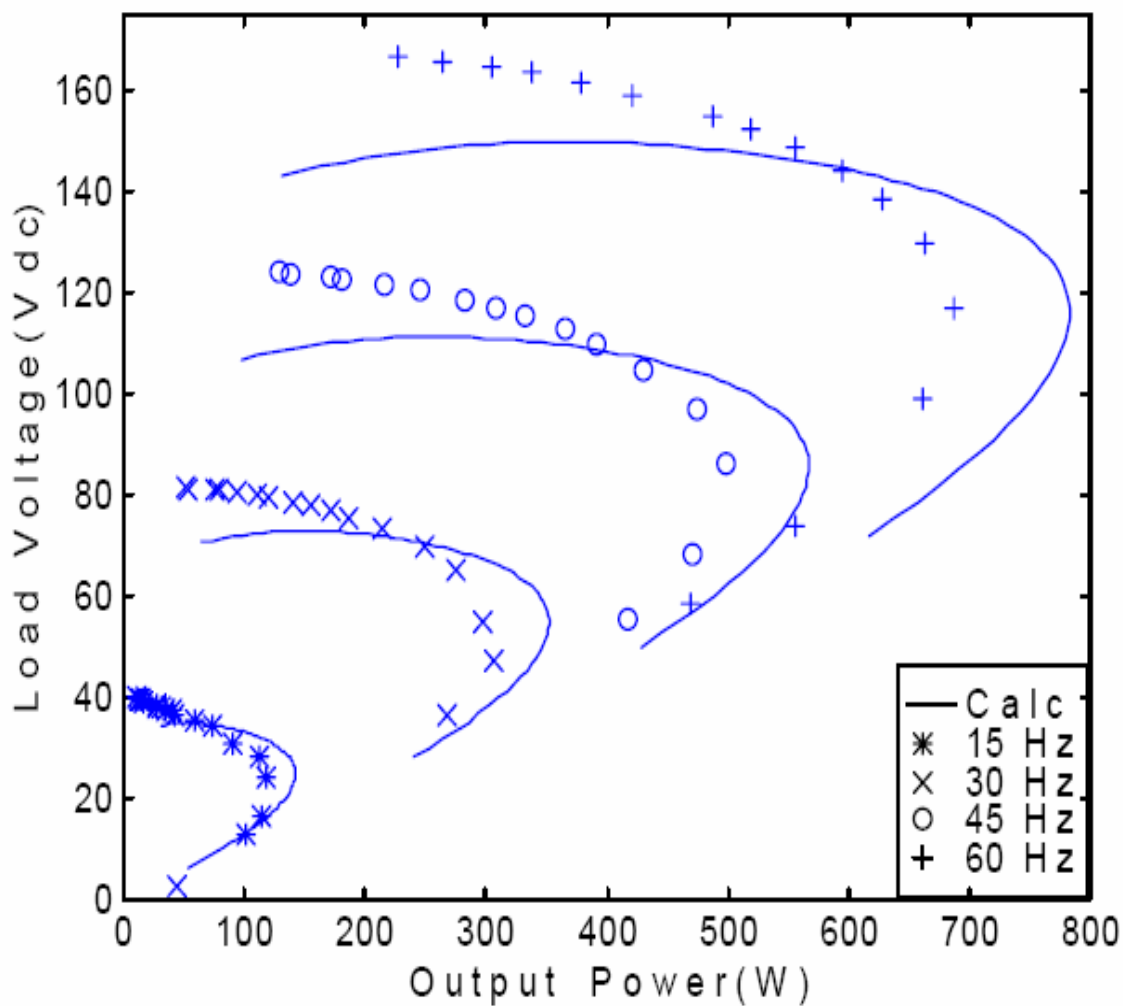
Figure 4.6. Measured and calculated load voltage vs generator output power

Finally, Figure 4.7 plots the measured power loss in the rectifier vs the load resistance. It can be seen that for all frequencies but 60 Hz, the loss in the rectifier is very small and, even for 60 Hz operation the loss is not that large. However, it must be remembered that the harmonics of the generator output voltage and current (caused by the rectifier) decreases the measured power going into the rectifier. Thus, in reality, the loss in power output due to the presence of the rectifier is much larger than the actual measured power loss between the input and the output of the rectifier.
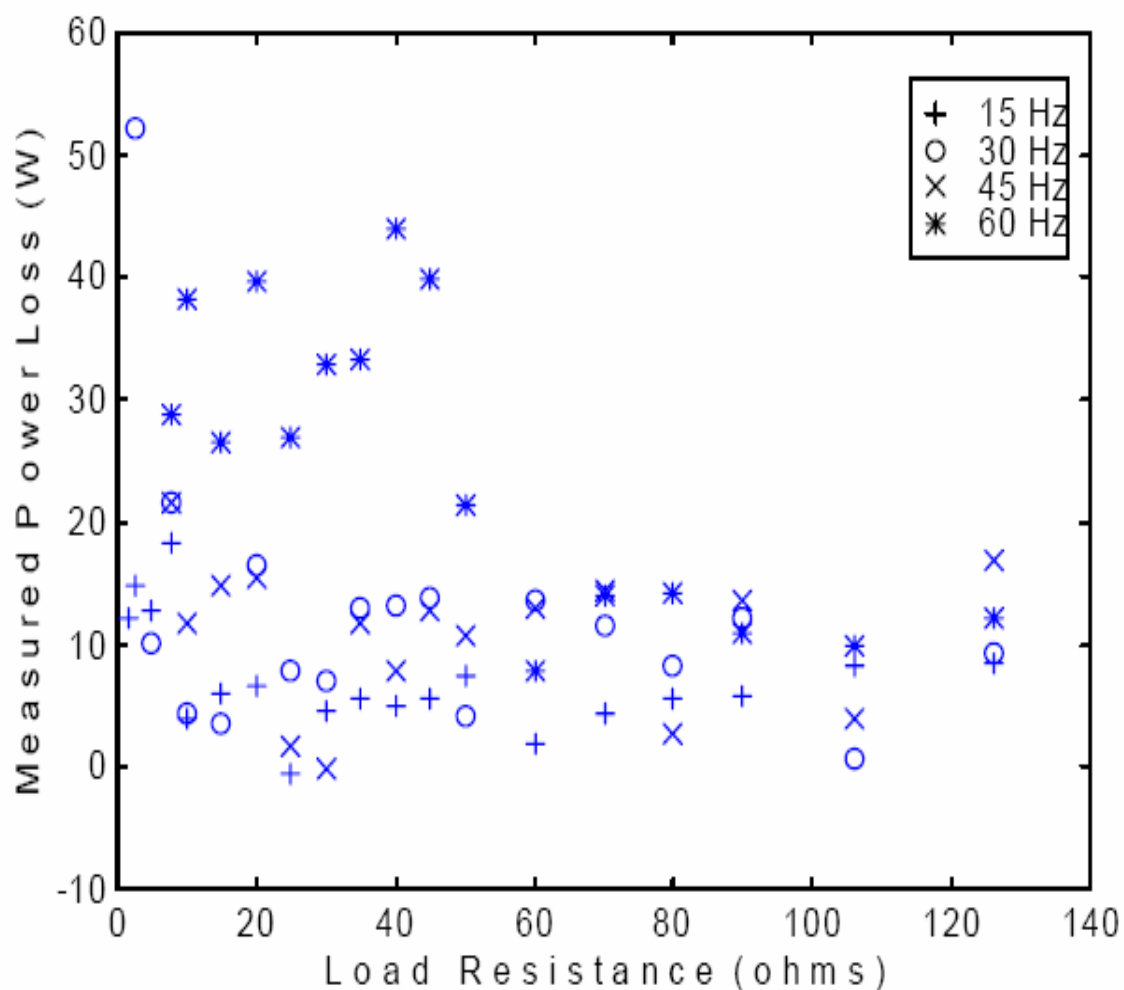
Figure 4.7. Measured power loss in the rectifier vs the load resistance

4.4. Modeling of the Diode, Capacitor, and Inductor

As was stated in the introduction of this chapter, the modeling of a diode switch is difficult. This is true because the diode turns on when the voltage across it is positive, but it will not turn off until the current flowing through it has become zero. The model of the diode, created by the authors of [30], is shown in Figure 4.8

The diode is modeled by an inductor in series with a nonlinear resistor.   The input into the block diagram shown in Figure 4.8 is the voltage across the diode U. The output is the current flowing through the diode I. The current flowing through the diode can be found by

$$I = \frac{1}{L_d} \int (U - R_D I)\, dt \ , \tag{4.32}$$

and this is exactly what the block diagram of Figure 4.8 is equating.   The nomenclature UI diode is a shorthand notation which   designates that the input to the diode is voltage and the output is current

Figure 4.9 shows how the feedback resistance is changed as the value of the current changes. The current out of the diode is fed into a switch which allows current to flow in R_{fwd} resistance (which has a mΩ value) as long as the current is positive; however, when the current becomes negative the switch causes current to flow in the resistor R_{rev} (which has a MΩ value) and essentially turns off the diode. The triangular boxes containing R_{fwd}
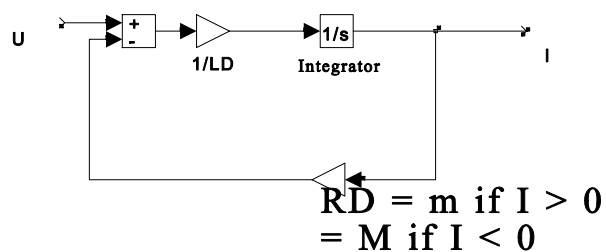
Figure 4.8. Resistive-Inductive model of a UI diode
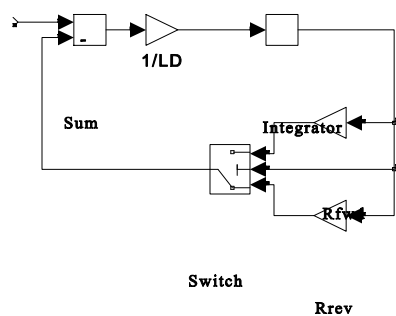
Figure 4.9. Simulink model of UI diode
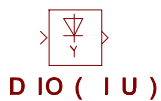
Figure 4.10. Simulink representation of a UI diode

and R_{rev} are gain boxes which multiply the input current by the respective values of resistance R_{Rev} and R_{fwd}. Figure 4.10 shows the symbol used to depict a UI diode.

There are two methods of creating a model of a diode which has current as its input and the voltage across it as its input. The first method is to use a differentiator instead of the integrator which was used for the UI diode. Using this method, one could create a block diagram to solve

$$U = L_d \frac{d}{dt} I + R_D I.$$
(4.33)

However, it is suggested in [30] that differentiating the input current introduces noise into the system. In order to avoid differentiating the input signal, the block diagram shown in Figure 4.11 is used. G is a very high gain and $H = I/V_{AK}$ (the transfer function of the UI diode).

The transfer function of the system of Figure 4.11 is

$$\frac{OUT}{IN} = \frac{G}{1 + G H} = \frac{G}{1 + G \dfrac{I}{V_{AK}}}.$$
(4.33)

For a very high gain, the transfer function can be approximated as

$$\frac{OUT}{IN} = \frac{G}{G \dfrac{I}{V_{AK}}} = \frac{V_{AK}}{I},$$
(4.34)
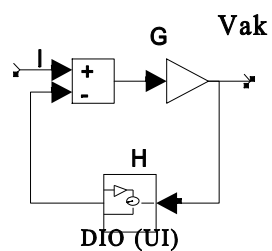
Figure 4.11. Simulink model of an IU diode

Figure 4.12. Simulink representation of an IU diode
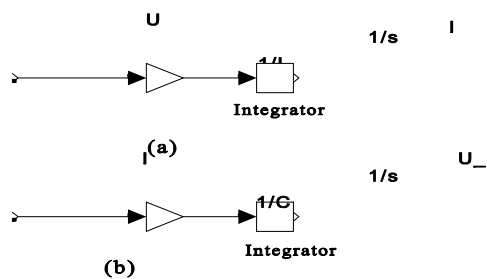
Figure 4.13. Simulink models of (a) a UI Inductor and (b) IU Capacitor

and, thus, a diode with current as the input and the voltage across it as its output has been created by using the topology shown in Figure 4.11. The symbol used for an IU diode is shown in Figure 4.12.

The modeling of a UI inductor and an IU capacitor are shown in Figure 4.13 These block diagrams solve the equations

$$I = \frac{1}{L} \int U \, dt$$
$$U = \frac{1}{C} \int I \, dt \ .$$

(4.35)

The models of the IU inductor and the UI capacitor are shown in Figure 4.14. These block diagrams solve the equations

$$U = L \frac{d}{dt} I$$
$$I = C \frac{d}{dt} U \ .$$

(4.36)

With the UI and IU diodes, it is possible to construct the full bridge diode with a LC filter feeding a resistive load shown schematically in Figure 4.15. The Simulink model of 3-phase full bridge rectifier is shown in Figure 4.16 and the model of the filter and load is shown in Figure 4.17. The power supply into the rectifier is a balanced 3 phase voltage source.
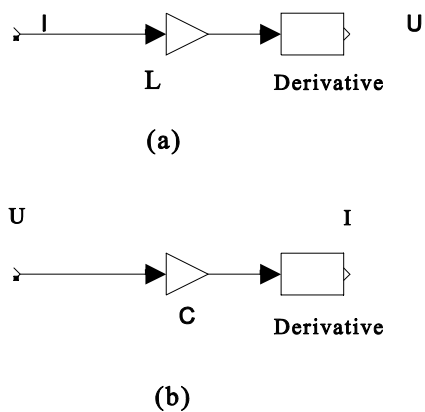
Figure 4.14. Simulink models of (a) an UI Inductor and (b) a UI capacitor
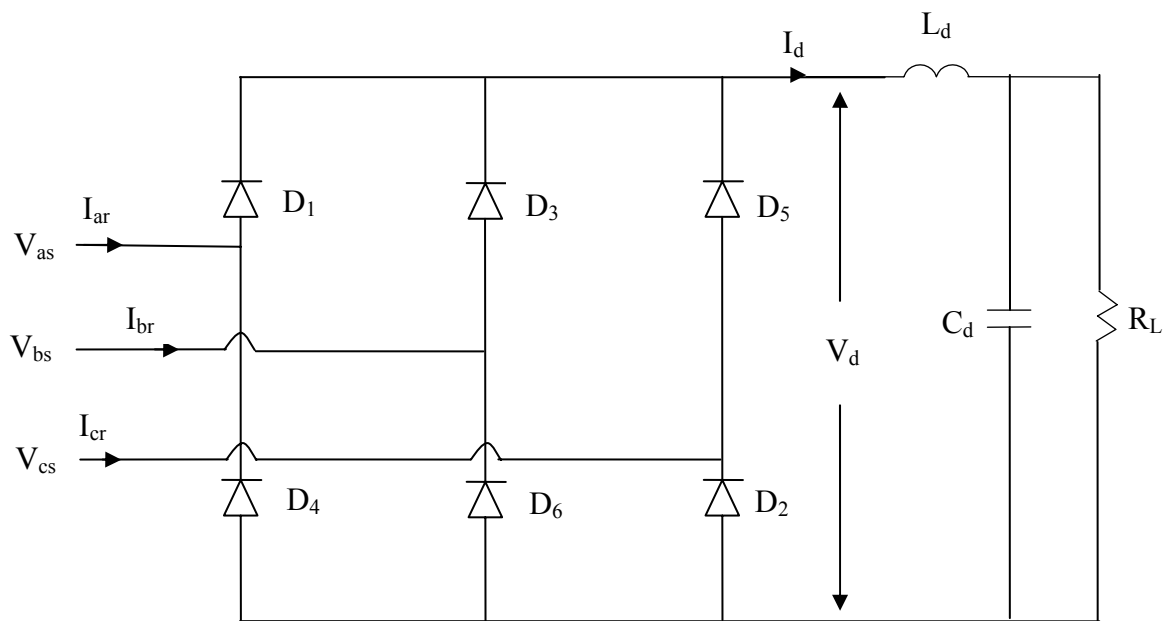
Figure 4.15. Schematic diagram of full bridge rectifier with filter feeding a resistive load
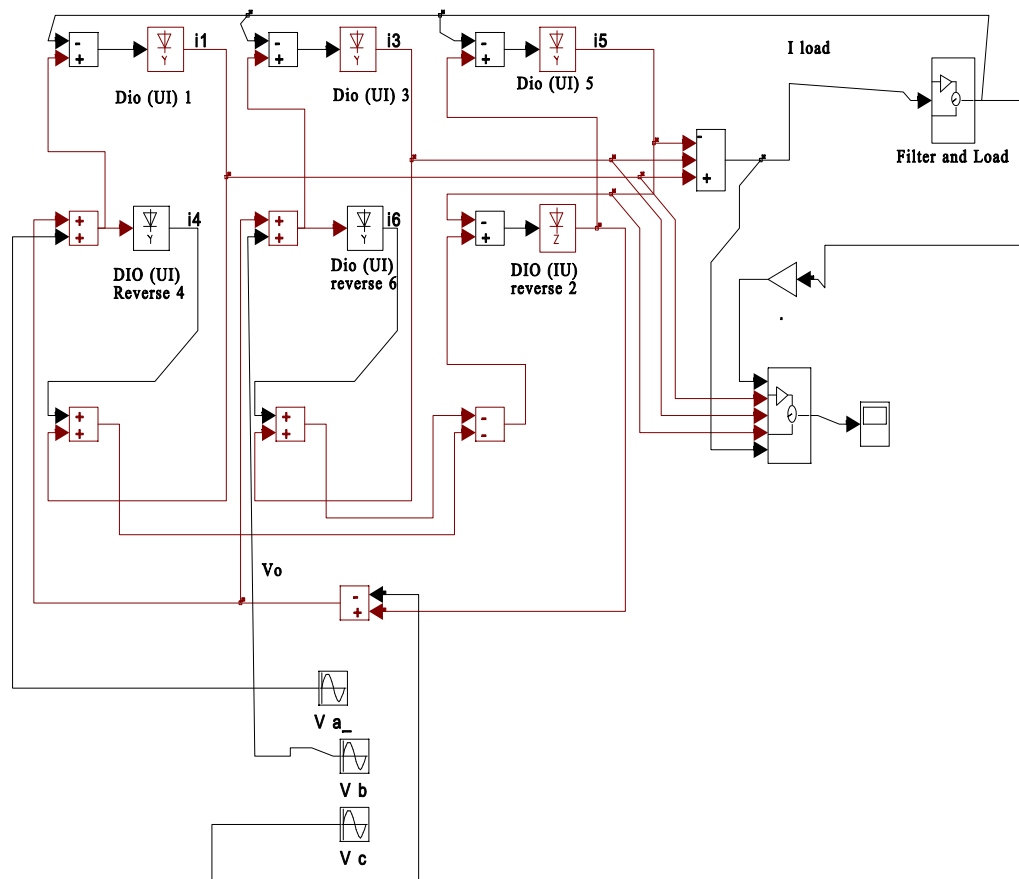
Figure 4.16. Simulink model of 3-phase full bridge rectifier with filter feeding a resistive load
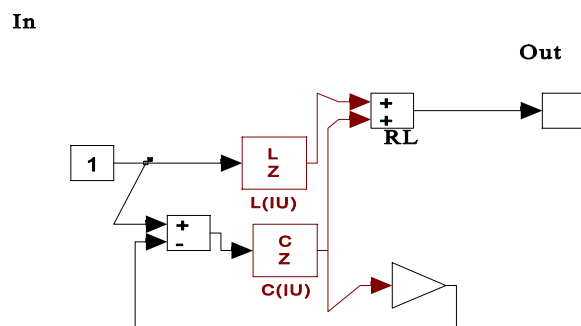
Figure 4.17. Simulink model of filter and resistive load

4.5 Simulation Waveforms of Ideal Voltage Source Feeding Full Bridge Rectifier

In this section, the simulated waveforms of the rectifier being fed by an ideal voltage source will be presented. This is done so that a comparison can be made between these waveforms and the waveforms found when the rectifier is being fed by the nonideal power source of the IPM machine. The magnitude of the line to neutral voltage source $V_{as,bs,cs}$ is 110 volts and is operating at 60 Hz. The filter inductor L_d has a value of 1 mH, the filter inductor C_d has a value of 100 µF, and the load resistance R_L has a value of 40 Ω.
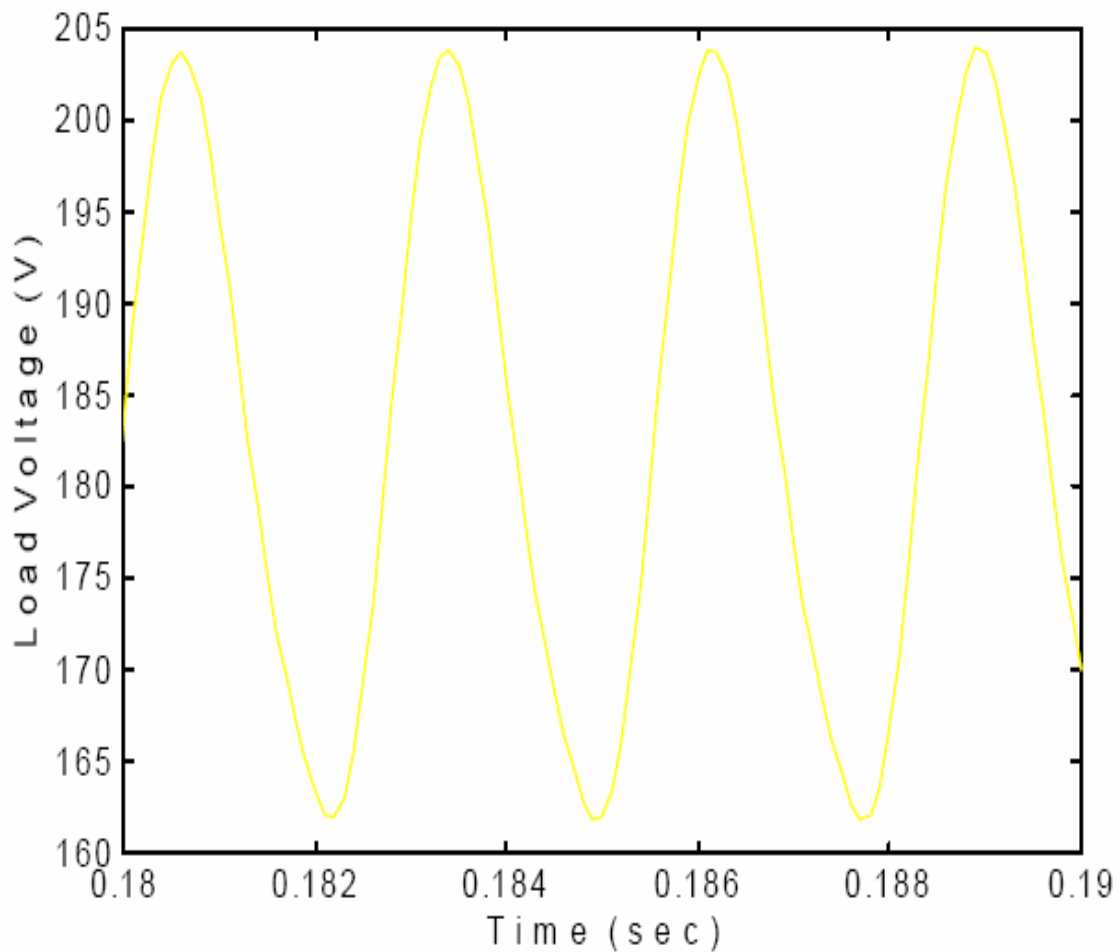
Figure 4.18. Load voltage vs time for ideal voltage source feeding rectifier
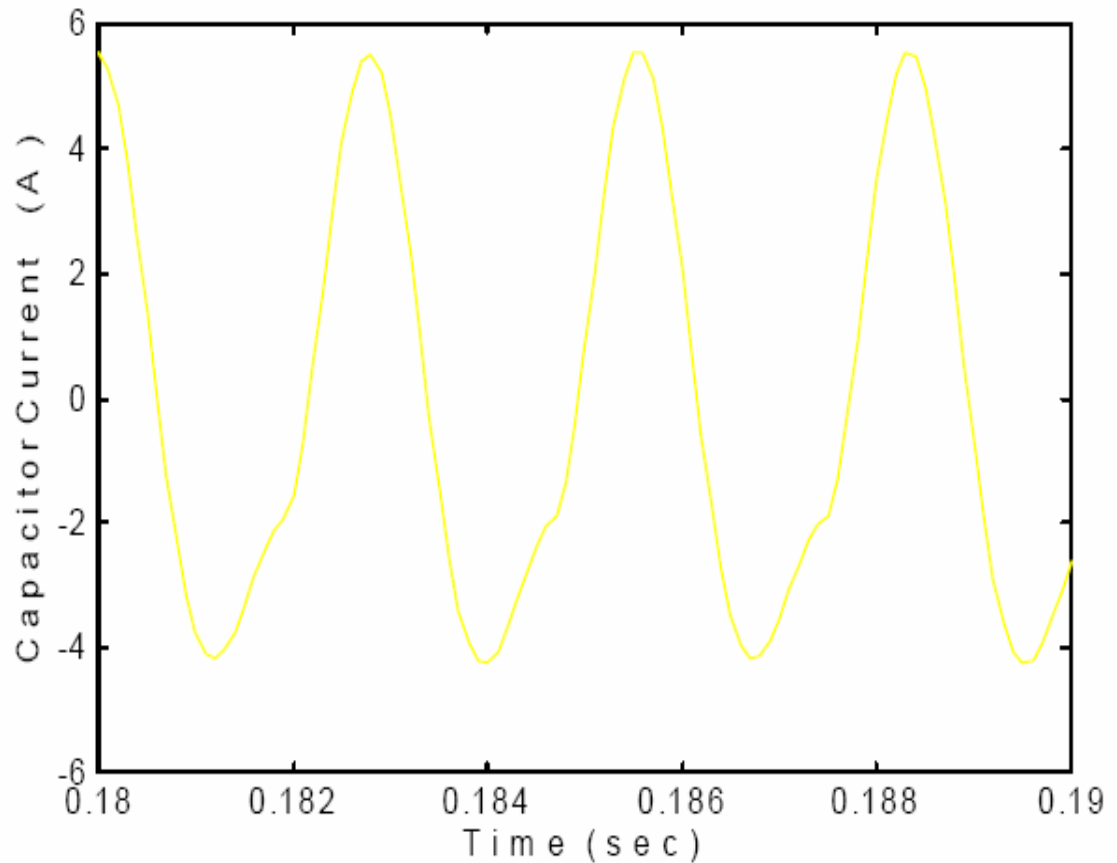
Figure 4.19. Simulated waveform of capacitor current vs time for ideal voltage source feeding rectifier

The voltage of the load is shown in Figure 4.18. It can be seen that there is a significant ripple voltage. This is due to the relatively small filter capacitor chosen in this simulation. It was stated previously that one advantage of using the ideal voltage source to feed the rectifier system was that it would be useful in filter design. A significant advantage of Simulink is that the parameters of the system can be changed while a simulation is running . The actual plots of any of the voltages and currents can also be observed during the simulation so that the affects of changing a particular parameter can be immediately seen. The current flowing through the capacitor is shown in Figure 4.19.

The current into the rectifier shown in Figure 4.20 is of particular interest. It can be seen that the waveform is not continuous (meaning that it has zero value for some period of time). Using the ideal voltage source scheme, the voltage waveform will obviously always be sinusoidal and, therefore, continuous. However, it will be seen in the simulation and measured waveforms of the IPM feeding the rectifier that the voltage and not the current is most often discontinuous.
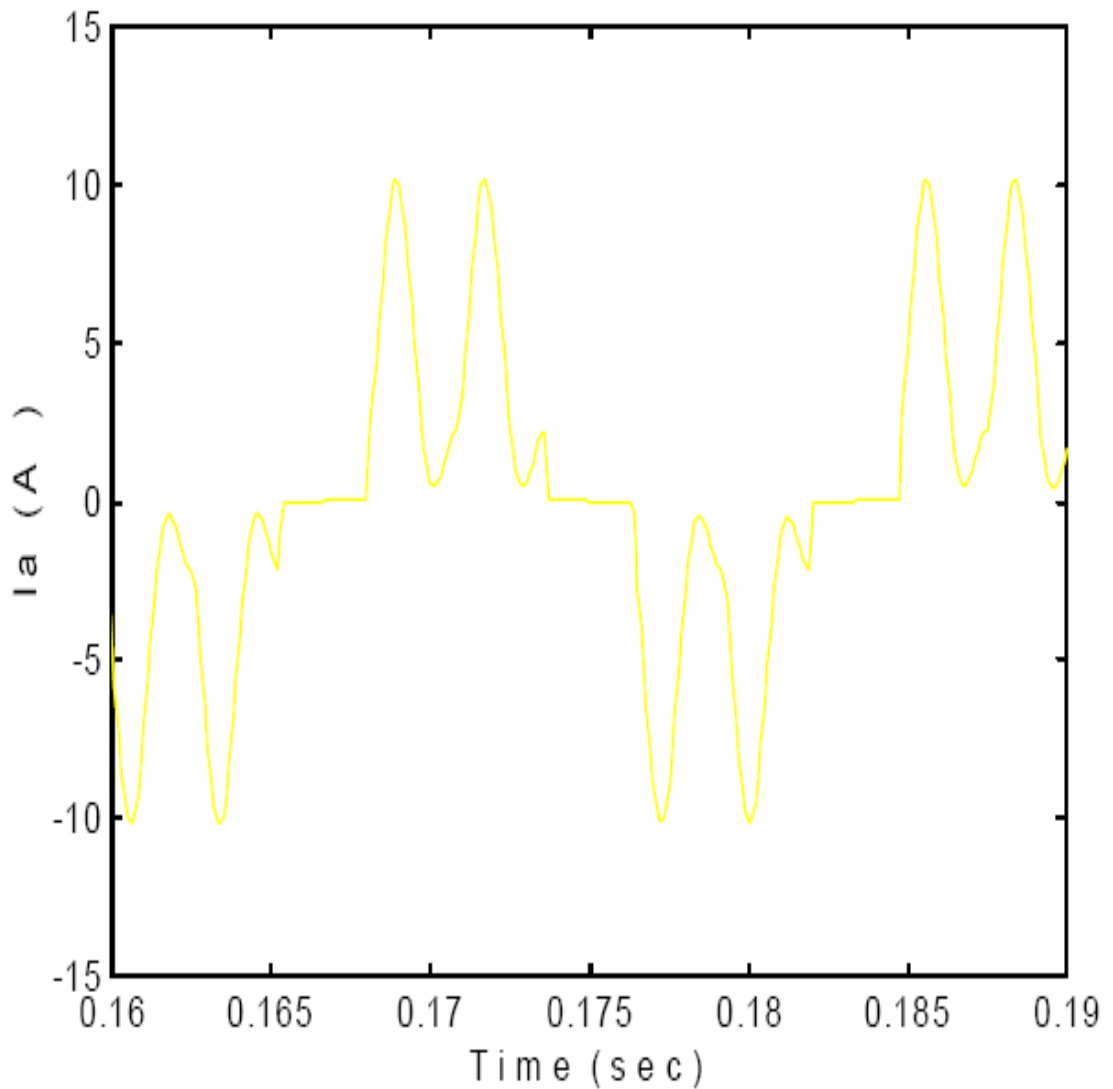
Figure 4.20. Simulated waveform of input current into the rectifier vs time

The current flowing through the inductor filter is shown in Figure 4.21. It can be seen that magnitude of the current varies from a peak of approximately 10 amperes to a minimum value of almost 0 amperes. The dip and rise of the inductor current corresponds to the "valley" seen between the peak points of the source current Ia. If the size of the inductor were increased, then both the inductor current and the source current into the rectifier would show less ripple.
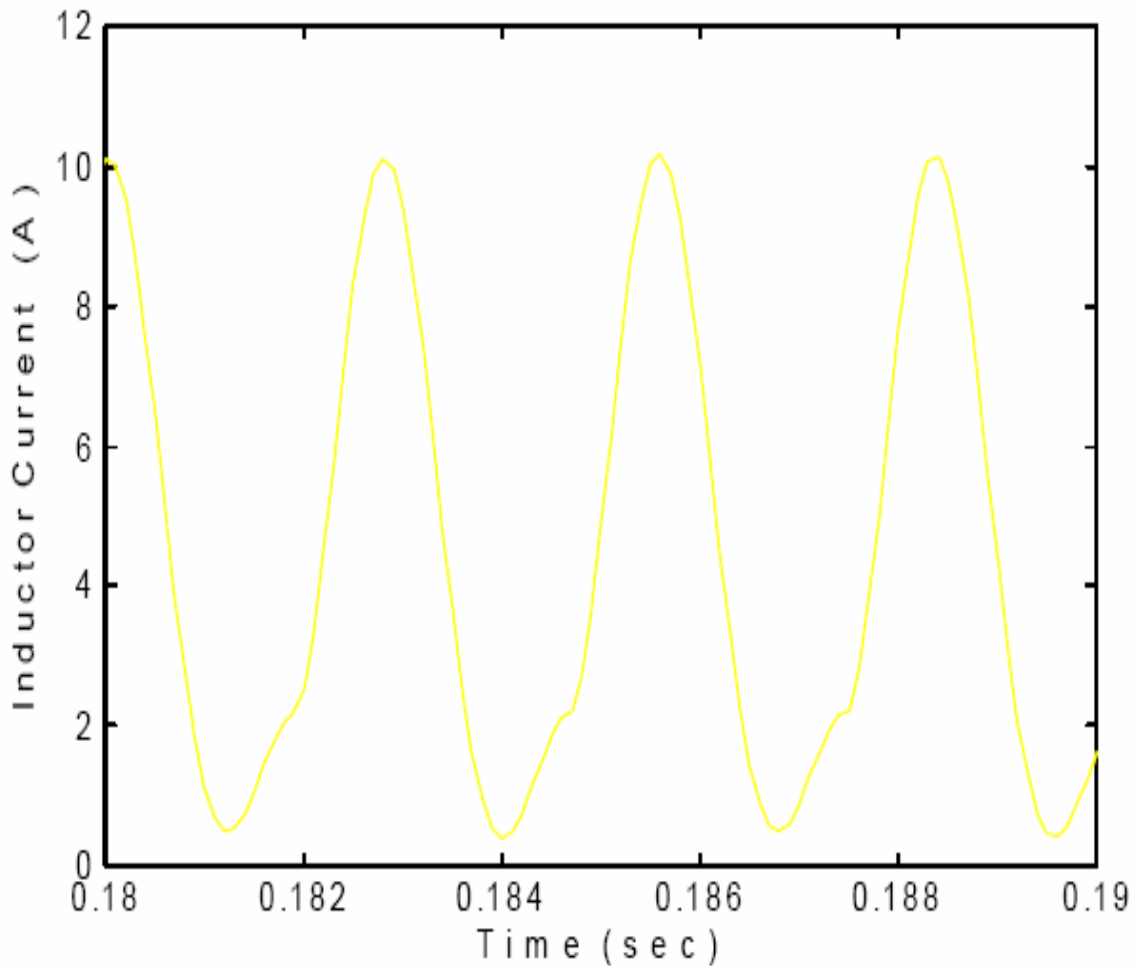
Figure 4.21. Simulated waveform of current flowing through the inductor filter for ideal voltage source feeding a rectifier

4.6 Comparison of Measured and Simulated Waveforms of IPM Machine with

Shunt Capacitive Compensation Feeding a Rectifier- Resistive Load

This section includes the comparison between simulation and measured waveforms for the IPM generator feeding a rectifier- resistive load. Shunt capacitors are used at the terminals of the generator to increase the power output and terminal voltage. Three cases will be looked at. The first is when the resistive load is such that high power is produced at the load, the second is when the resistive load is very high and little power flows in the load. The third case is for the same high resistor and a higher value for the rectifier filter capacitor. It will be shown that increasing the filter capacitor causes oscillations in the system.

4.6.1 IPM Generator Feeding a Small Resistive Load

This section looks at measured and simulated waveforms when the IPM is operating at near its maximum power output point. All of the waveforms in this and the next two sections are at the frequency of a 45 Hz. Since the IPM is a 4 pole machine, then this means that the shaft speed is 1350 rpm. The load resistance for the waveforms presented in this section is 22 Ω. The rectifier inductor is 10 mH and the filter capacitor is 5.8 μF.

Figure 4.22 shows the simulated and measured line to line voltage waveforms for the 22 Ω load. It can be seen that in both the simulated and measured waveforms that there is a deadband in which the line to line voltage is zero due to the commutation overlap. This
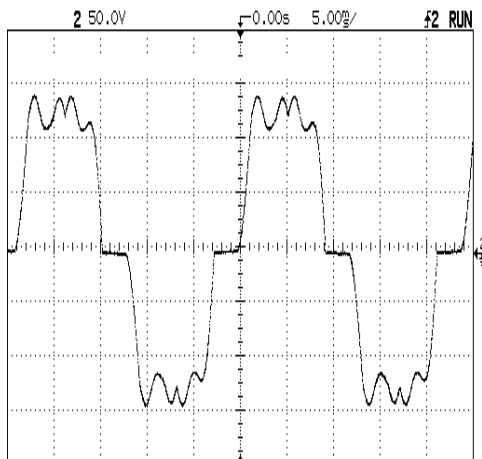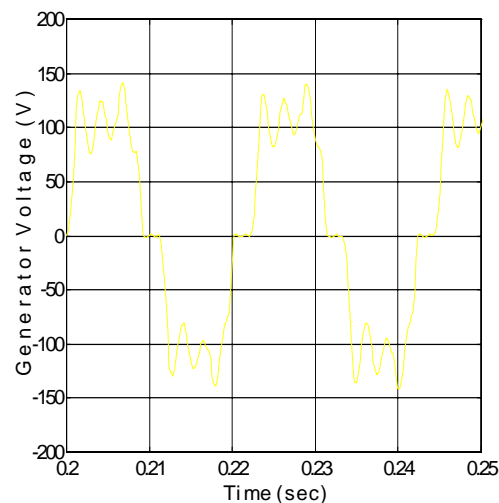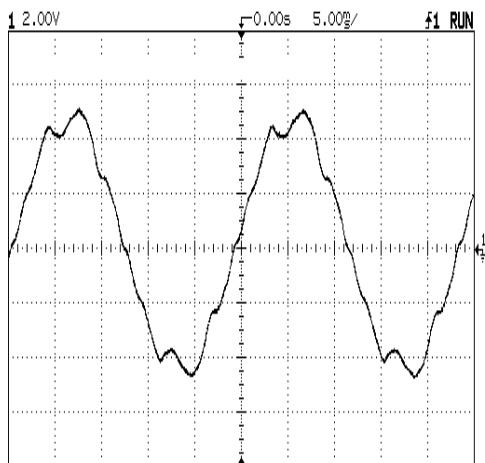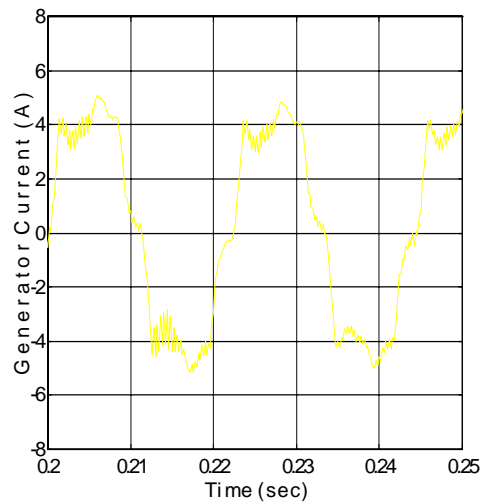
I. Measurement   II. Simulation

Figure 4.22. Measured and simulated line to line voltage waveforms for the generator feeding a rectifier-resistive 22 Ω resistive load. Rotor speed=1350 rpm.   Measured waveform scale: voltage: 50v/div, time 5ms/div

does not mean that the phase voltages are zero in this dead band - rather it means that the voltage of phase a equals the voltage of phase b.   Comparing the voltage waveforms for the rectifier case with the voltage waveforms when the IPM is feeding the resistive load (see Figure 3.15) it can be seen that the waveforms of Figure 4.22 have significantly more harmonics in them.

Figure 4.23 shows the measured and simulated waveforms of the generator current. Like the measured voltage waveform, it can be seen that the generator current for both the simulated and measured waveforms have significantly more harmonics present than was the case for the IPM feeding a purely resistive load. See Figure 3.16. The comparison between the simulated and measured waveforms is favorable in both magnitude and form.

I. Measurement   II. Simulation

Figure 4.23. Measured and simulated generator currents waveforms for a 22 Ω load. Rotor speed=1350 rpm. Measured waveform scale: current 2A/div, time 5ms/div
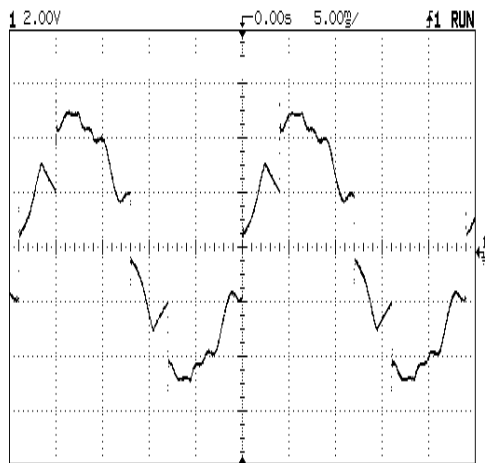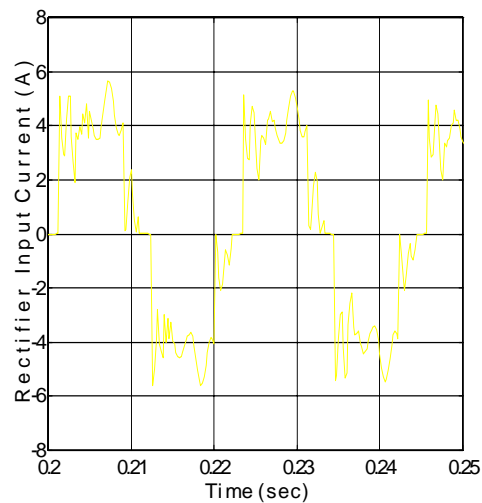
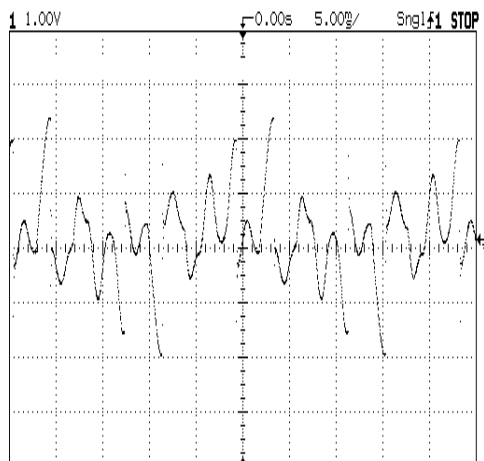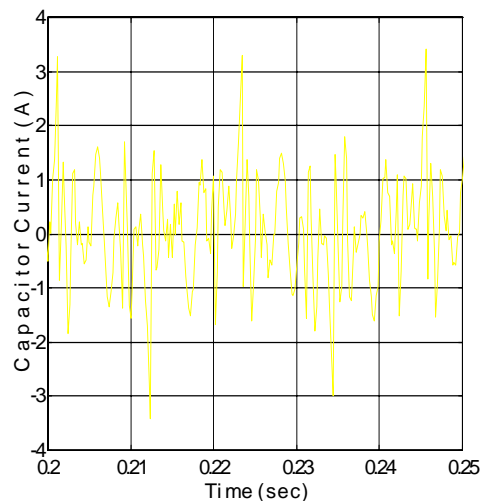
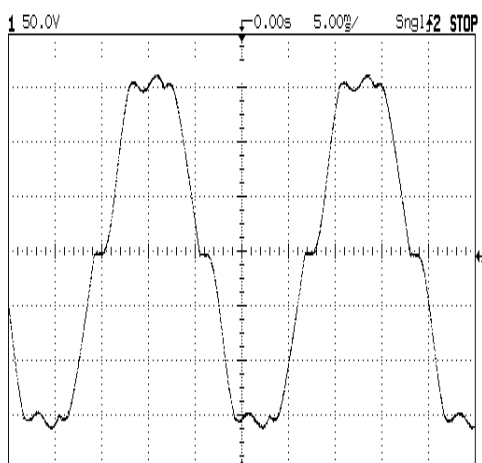I. Measurement   II. Simulation

Figure 4.24. Measured and simulated rectifier input currents for a 22 Ω rectifier-resistive load. Rotor speed=1350 rpm. Measured waveform scale: current: 2A/div, time 5ms/div

I. Measurement   II. Simulation

Figure 4.25. Measured and simulated capacitor currents for a 22 Ω rectifier-resistive load. Rotor speed=1350 rpm. Measured waveform scale: current:1A/div, time 5ms/div

The measured and simulated waveforms of the current flowing into the rectifier are shown in Figure 4.24 Again, the measured waveform shows a slight distortion, but the simulated and measured waveforms are reasonably close

Finally, Figure 4.25 shows the measured and simulated waveforms of the current flowing through one of the ac side capacitors. It can be seen that the average of this current is zero and that the frequency of oscillation about zero is very high.

4.6.2 IPM Generator Feeding a Large Rectifier- Resistive Load

In this section, measured and simulated waveforms for the condition of a 132 Ω load are discussed. The operating frequency is 45 Hz and the shunt capacitors are Y-connected 30 μF.
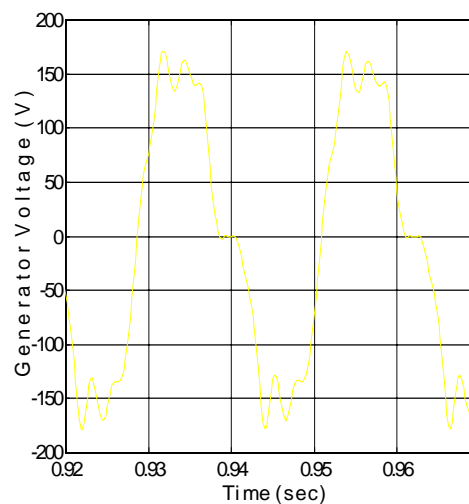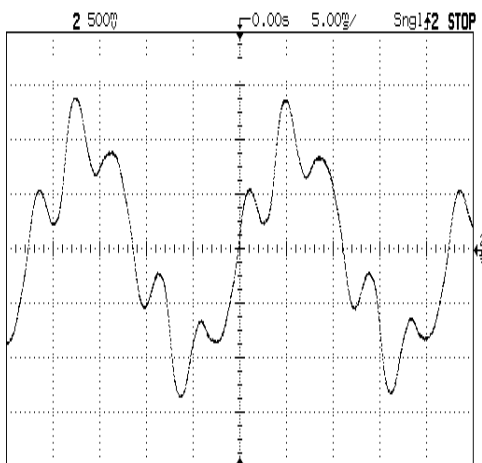
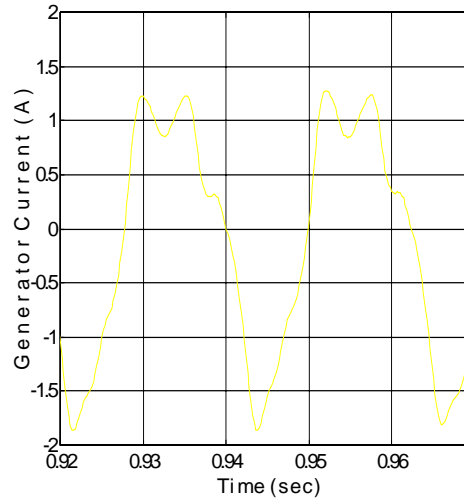I. Measurement   II. Simulation

Figure 4.26. Measured and simulated waveforms of the line to line voltage for a 132 ohm rectifier-resistive load. Rotor speed = 1350 rpm. Measured waveform scale: voltage: 50v/div, time 5ms/div
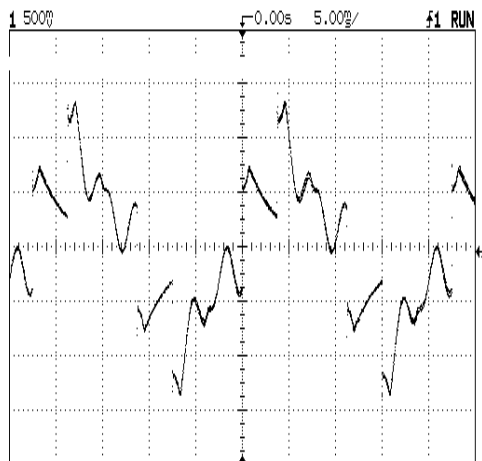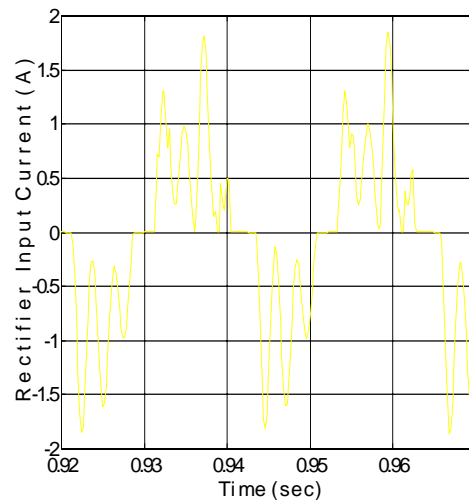

I. Measurement   II. Simulation

Figure 4.27. Measured and simulated waveforms of the generator line current for a 132 ohm rectifier-resistive load. Rotor speed = 1350 rpm. Measured waveform scale: current: 500mA/div, time 5ms/div

Figures 4.26 - 4.29 plot the measured and simulated line to line voltage and current out of the generator, current into the rectifier, and current through the a.c. capacitor for the case when the IPM generator is feeding a very light load. While the simulated and measured waveforms of the line to line voltages compare favorably for the light load condition, it can be seen that there is a definite difference between the simulated and measured waveforms of the generator and rectifier current waveforms. It is believed that much of the reason for this is that, since there is an exponential rise in the d and q axis inductances at light load, any error in the curve fit or machine parameter determination is magnified.
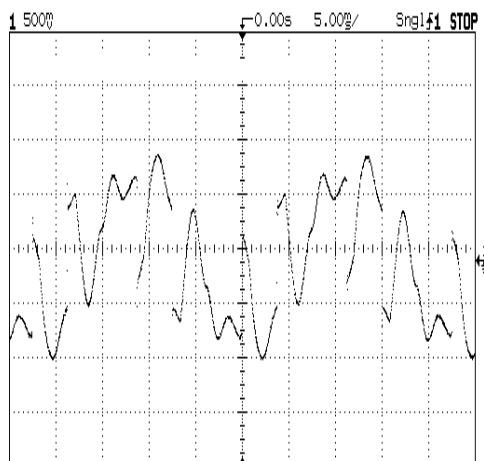

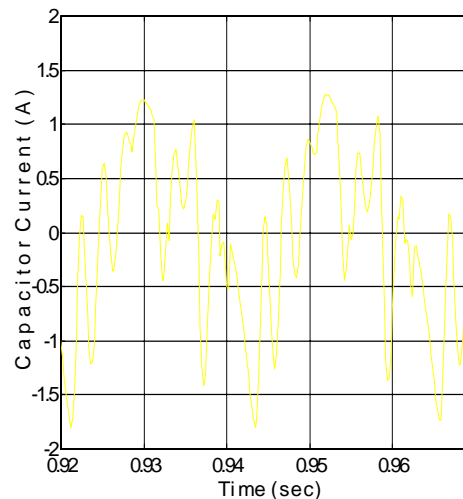I. Measurement   II. Simulation

Figure 4.28. Measured and simulated waveforms of the input rectifier   current for a 132 ohm rectifier-resistive load. Rotor speed = 1350 rpm. Measured waveform scale: current: 500 mA/div, time 5ms/div
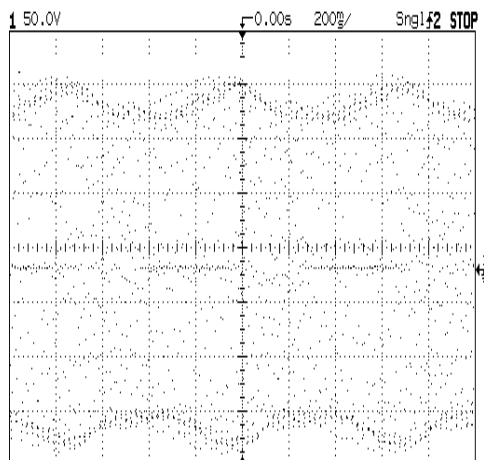
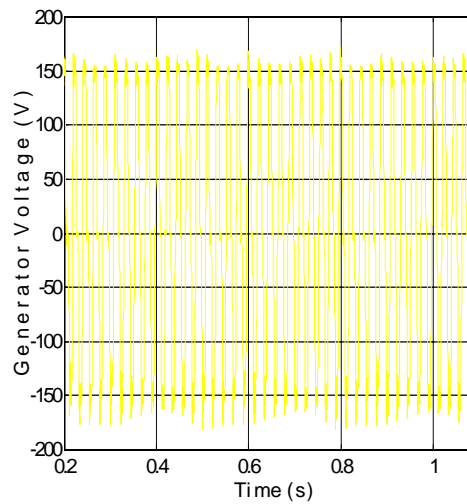|	
I. Measurement	II. Simulation

Figure 4.29. Measured and simulated waveforms of the a.c. capacitor current for a 132 ohm rectifier-resistive load. Rotor speed = 1350 rpm. Measured waveform scale: current: 500 mA/div, time 5ms/div

4.6.3 IPM Generator Feeding a Large Rectifier- Resistive Load and Undergoing Quasi-Periodic Subharmonic Oscillations

In this section, measured and simulated waveforms for the conditions exactly the same as those of section 4.6.2 are presented- except that the rectifier capacitor is changed from 5.6 µF to 11.2 µF. It will be seen that this change causes dramatic changes in how the system behaves. Figures 4.30 - 4.31 show that the line to line generator voltage and the generator current are oscillating from relatively small values to larger ones. The effect is more pronounced in the generator current. Although the y axis of the simulated and measured waveforms is the same, the time axis is not.
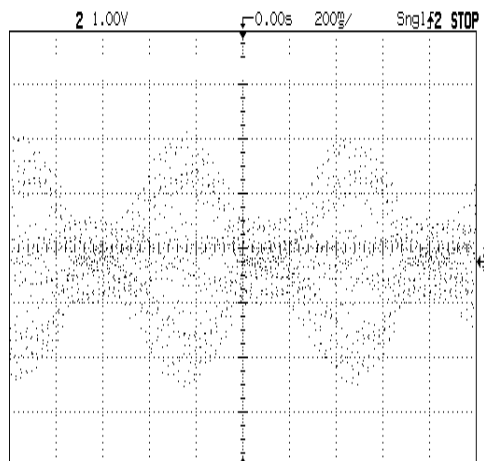
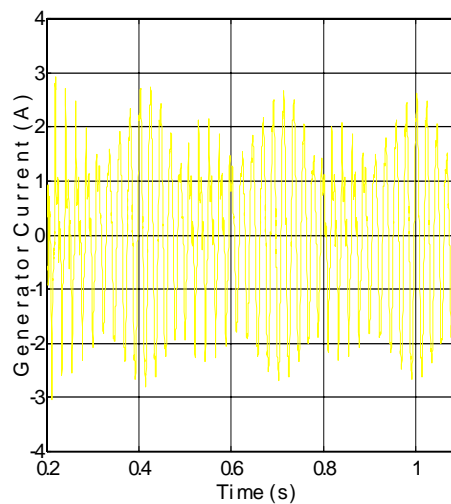I. Measurement   II. Simulation

Figure 4.30. Measured and simulated waveforms of the line to line generator voltage   for a 132 ohm rectifier-resistive load.   Rotor speed = 1350 rpm. Measured waveform scale: voltage: 50 V/div, time 5ms/div

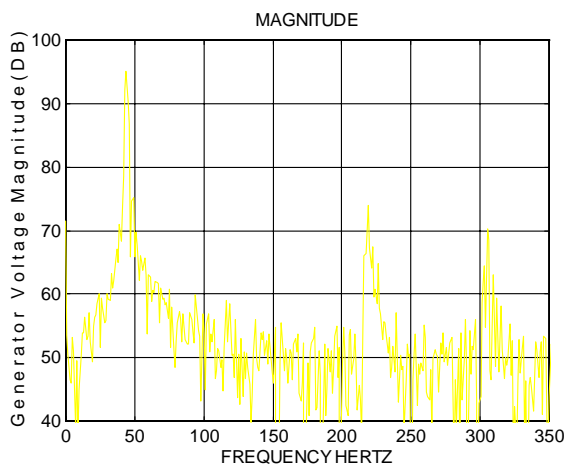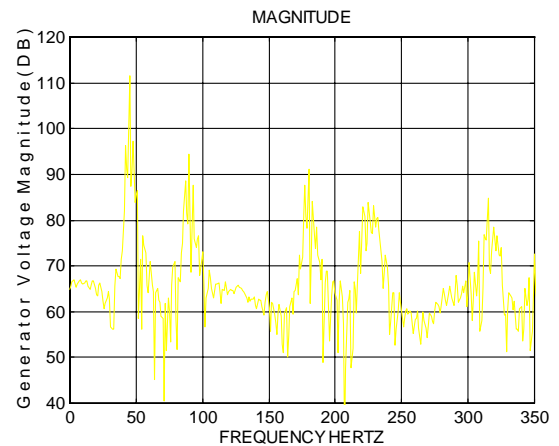I. Measurement   II. Simulation

Figure 4.31. Measured and simulated waveforms of the generator current   for a 132 ohm rectifier-resistive load.   Rotor speed = 1350 rpm.   Measured waveform scale: current: 1A/div, time 5ms/div

The reason for this is that for these parameters, the Simulink program would always stop before 1.1 seconds. Much effort was devoted to solving this problem, but the attempt was unsuccessful.

The fast Fourier transforms of the generator voltages and currents are given in Figures 4.32 and 4.33, respectively. It can be seen that the measured FFT shows the fundamental 45 Hertz component and two higher order components at approximately 220 and 305 Hertz.
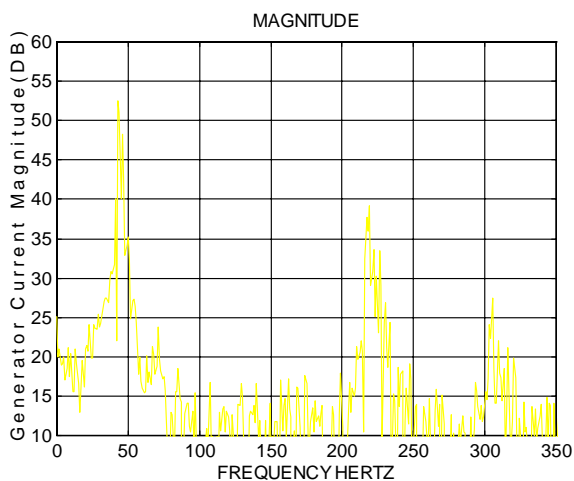

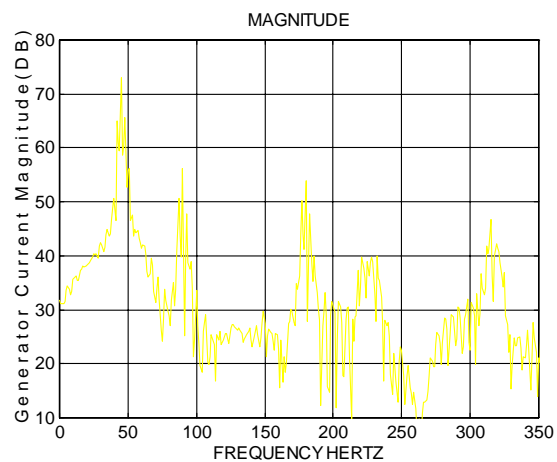I. Measurement   II. Simulation

Figure 4.32. Fast Fourier transform of measured and simulated waveforms of the generator line to line voltage   for a 132 ohm rectifier-resistive load. Rotor speed = 1350 rpm
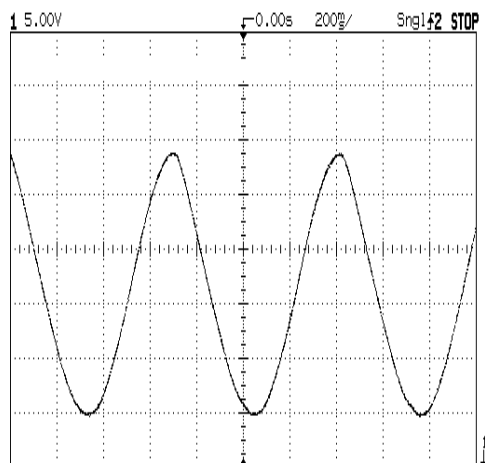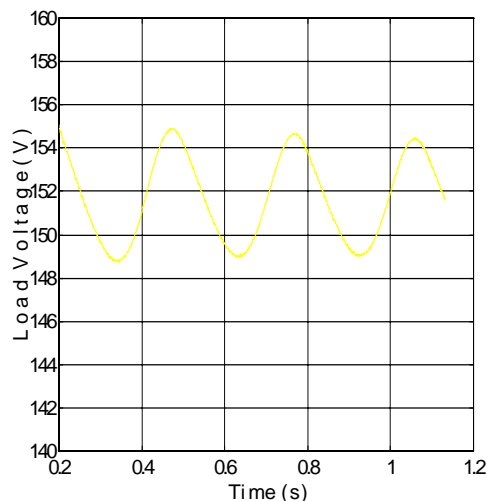
I. Measurement   II. Simulation

Figure 4.33. Fast Fourier transform of measured and simulated waveforms of the generator line current   for a 132 ohm rectifier-resistive load. Rotor speed = 1350 rpm

Although the FFT shows the higher order harmonics, the graphs of Figures 4.32 and 4.33 do not tell the complete story because there is a subharmonic oscillation which does not appear on the graphs. Referring to the measured waveform of Figure 4.31, and noting the time scale is 0.2 seconds per division, it can be seen that the magnitudes of the generator currents repeat themselves approximately every 0.68 seconds. This is the same frequency of oscillation of the load voltage, as   can be seen in Figure 4.34.   It should be noted that the simulated waveforms are oscillating at the much faster rate of about 0.35 seconds for each cycle (about twice as fast as the actual measured waveforms).

I. Measurement   II. Simulation

Figure 4.34.   Measured and simulated waveforms of the load voltage   for a 132 ohm rectifier-resistive load. Rotor speed = 1350 rpm. Measured waveform scale: voltage: 5V/div, time 200ms/div

There are several possible reasons for the differences in the simulated and measured waveforms for this oscillatory case. The first reason is that, as was seen in section 4.62, the waveforms of the measured and simulated waveforms were not exactly the same even when no oscillation was occurring. The second reason is that the model used to describe the IPM did not take into account the presence of the damper windings in the rotor. During normal steady state operation, neglecting the damper windings is appropriate; however, the damper windings will have an effect when the voltages and currents are oscillating in the fashion depicted in this section.